

Superregenerative Receivers for Remote Keyless Access Applications

A high performance low-cost design approach for wireless activation

By Stuart Rumley

The superregenerative receiver (SRR) is one of the oldest receiver technologies still in widespread use today¹. Perhaps more SSRs are in use today than all other receiver type combined. SSRs are used in very large volume applications such as perimeter detection alarms and remote meter reading devices. Perhaps the most well know application is in remote keyless entry devices used for automobile door, garage door and gate openers. This paper provides a reference design for a modern, high performance, low cost SRR suitable for keyless entry applications.

Background

Superegenerative actually refers to the type of detector that the receiver uses to detect and demodulate the baseband signal. The standard superhetrodyne receiver used for A.M. broadcast reception typically uses some form of diode detector to perform envelope detection in order to recover the analog audio baseband signal. However, it is possible, but not necessarily desirable, to replace the diode detector with a superegenerative detector. The superegenerative receiver is actually an evolution of the regenerative receiver. In the early years of radio, vacuum tubes were scares and expensive. Tuned radio frequency (TRF) receiver topologies where the common topology of the day. These receivers comprised of usually three vacuum tube RF amplifiers followed by a vacuum tube diode detector stage and a two or more vacuum tube audio stages. Because of the nearly infinite gain attainable in a single stage, the regenerative receiver could replace most of the tubes with a single tube at considerable savings. Consequently, the regenerative receivers where quite popular particularly with amateur radio operators and electronic experimenters.

The regenerative receiver must not have been very popular with the average consumer, however, who was more interested in listening to the radio broadcast than fiddling with the technology. The regenerative receiver required that the operator constantly adjust the feedback or "regen" knob in order to bring the detector to the verge of oscillation. Too much feedback and the receiver would howl violently, too little and weak signals would not be received.

The SRR solved this problem by automatically increasing the gain of the detector stage until oscillation just started. As soon as the oscillatory condition started the bias conditions would change and the oscillation would cease or "quench". This process would continuously bring the detector into its most sensitive region at a rate that was higher than the audio frequency range (hence the term super as in supersonic) but lower than the radio frequency range.

The major advantage then, as it is today, of SRR is its low cost. With the exception of single solid state diode detector, the SRR remains the lowest cost receiver topology available today. Moderate volume (10K units) production cost for fabrication and assembly of these receivers can be well under \$3.00 (U.S. 1996) . When integrated into a complete keyless entry system the cost of the receiver section could easily be under \$2.00.

Another significant advantage of the SRR is its low power consumption. An externally quenched SRR operating with a current controlled RF stage can be operated at 3 Volts with less than 10uA average current drain. This type of power consumption would allow battery powered receivers to operate in the field for many years.

The disadvantages of the SRR are:

- Poor selectivity resulting in possible interference from an adjacent channel.
- Susceptibility to front end overload. Strong local signals on frequencies far removed from the operating frequency of the SRR can desensitize the receiver.
- Limited to amplitude modulation modes.
- Frequency stability. Frequency accuracy and stability is determined by the tuned circuits in the detector as well as the temperature stability of the detector transistor parameters.

Receiver Design

Superregens are clearly unique and probably the least understood of all the receiver topologies. Much has been written on the subject of regenerative and superregenerative receivers in previous works and the theory is covered in detail in the references provided². However, a good engineering analysis of the circuit designs concepts remains scarce. I believe this is due as much to the highly competitive nature of the commercial applications, as it is to the complexity and dynamics of the detector's operation.

The superregenerative detector stage operates simultaneously at three frequencies: one is typically a VHF radio frequency, another is the super sonic quench frequency, and the third is the audio or baseband data frequency. The RF frequency of interest is amplitude modulated and will have a signal level -30 to -100dBm. The quench frequency will be simultaneously changing the bias, and as a result the gain, over a very large range including off. All of these disparate frequency and amplitude consideration defy simulation with most current software tools making circuit design and performance prediction extremely difficult.

The simulation tools that the modern radio designer has available fall into three categories: 1) Linear simulators such as Eagleware³, 2) non-linear simulators such as PSPICE⁴ and 3) advanced work station non-linear simulators such as Hewlett Packards MDS or Microwave Harmonica⁵. Linear simulators will not be able to deal with the bias changes cause by the quenching action nor will they be able to predict the onset of the RF oscillation. SPICE simulators should be able to model the function but a huge number of samples would be required with very short sample periods in order to capture all three frequencies of interest. It is doubtful that the data obtained with SPICE methods could be used productively. The work station simulators, while possessing the capability, require a great deal of knowledge and experience to set up properly for accurate results. In any event I highly doubt that even the best methods available could predict the circuit operation with the degree of certainty that would be required in order to optimize a design for maximum sensitivity, lowest power, or frequency stability.

Figure 1 is the block diagram of SSR described in this paper. The major blocks are:

- The input buffer RF amplifier.
- The superregenerative detector.
- Detector and amplifier low pass filters.
- Base band audio frequency amplifier.

- Voltage comparator.

The input buffer RF amplifier establishes the noise figure for the receiver which is an

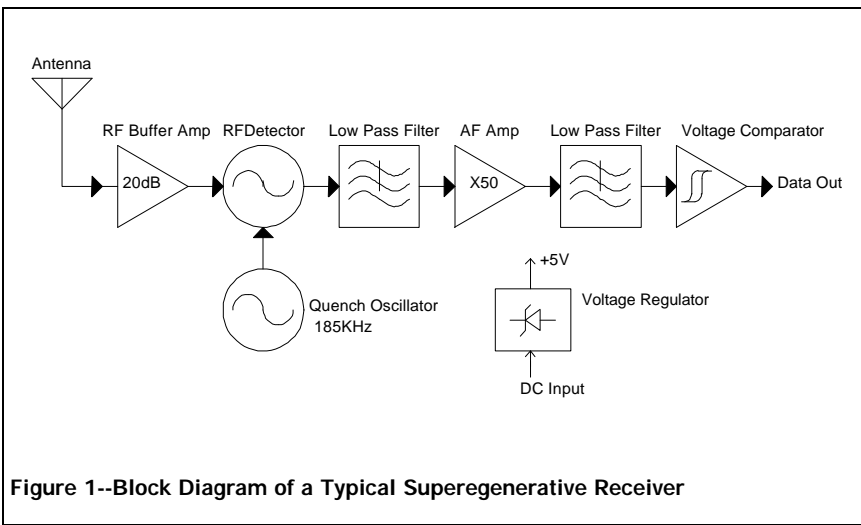


Figure 1--Block Diagram of a Typical Superregenerative Receiver

important parameter in determining the ultimate sensitivity and range performance. The RF buffer amplifier also isolates the following RF detector stage from the antenna. Isolation is required in order to prevent RF energy created by the detector RF oscillations from being radiated by the antenna and

violating FCC part 15 regulations. Further more, the buffer amplifier prevents impedance variations in the antenna caused by changes in the nearby environment from pulling the RF detector frequency and subsequently resulting in a loss of sensitivity. The gain provided by this stage is should be from 10 to 20dB.

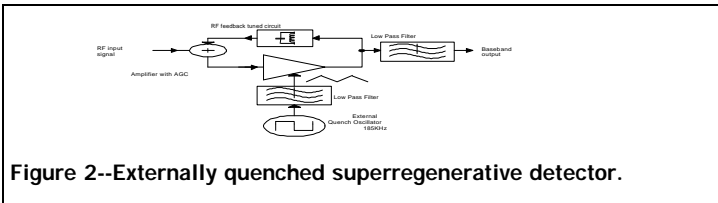


Figure 2--Externally quenched superregenerative detector.

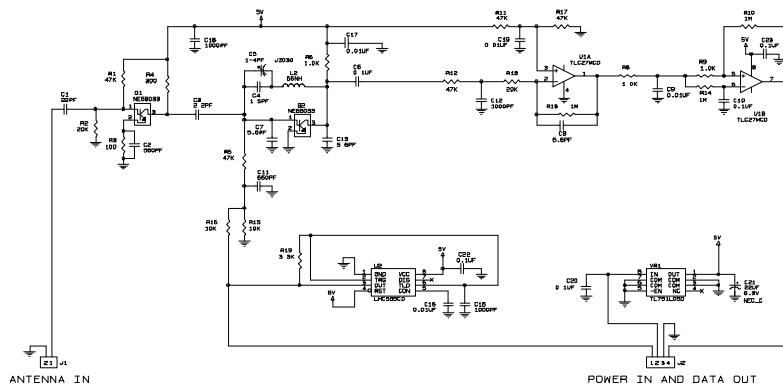
The output of the input RF buffer amplifier is coupled to the superregenerative RF stage. A more detailed functional block diagram of the detector is shown if figure 2. The detector

essentially functions as an RF amplifier with and AGC port. A tuned circuit provides positive feedback at the RF frequency from the output to the input of the RF amplifier. Added to the feedback signal is the coupled RF input from the buffer amplifier. The AGC port is driven from a triangle waveform derived from the external quench oscillator and lowpass filter. The gain of the RF amplifier is varied by the AGC signal from zero to its maximum value. At some point, as the gain is increased, the Barkhausen criterion* will be satisfied and the detector will break into oscillation.

Detailed Circuit Description

* For oscillation to occur in a network the phase of the loop gain must be zero and the magnitude of the loop gain must be unity.

The complete circuit schematic diagram of the receiver is shown in figure 4. Q1 is input RF amplifier/buffer transistor. The antenna signal is coupled by C1 directly to the base of Q1 without the benefit of any tuned circuits. R1, R2, and R3 determine the bias conditions for Q1. This stage draws approximately 7mA. of current and is largest current consumer in the receiver. R4 is the output load and sets the broadband band gain of this stage. This stage provides approximately 20dB of gain at the operating frequency. It may seem desirable to place a tuned circuit in the RF amplifier but it really is not needed. The SRR is only responsive at the frequency that the detector is operating at, in this case 418MHz. There is no image frequency or higher order mixer spurious responses to be concerned about. And because the amplifier is biased at a relatively high level (7mA.) it will not be particularly susceptible to front-end overload. This should hardly ever be a problem so long as only 1/4λ antennas (i.e. no high gain yagis at 100') connected at the receiver board are used. It should be noted, however, that the SRR is weakly responsive to strong signals at one-half the operating frequency (209MHz). If this should ever become a problem, a simple L/C series trap could be installed directly at the antenna



The RF amplifier is coupled to the detector, through C3. The detector consist of Q2 and its surrounding tuned circuit, C13, L2, C5 in parallel with C4 and C7. Q2 provides the necessary gain and a phase shift of 180°. The π-network formed by C13, L2, and C7 produce an additional 180° of phase shift,

thus satisfying the required 360° for sustained oscillation. The series combination of C4 in parallel with trimmer C5 and L5 form the net inductive element of the π-network. C5 is then used to set the detector on frequency. You can estimate the frequency of operation for

the detector from the formula: $f_{det} = \frac{1}{2\pi \sqrt{\frac{C5 \cdot C4}{C5 + C4} \cdot L2}}$. A linear simulator can be used

to analyze the frequency of operation of the detector circuit by considering it a loop oscillator. This will not yield any insight into the actual detector operation, but will provide an understanding of the VHF oscillator.

The inductor used in this circuit is an 0805 surface mount inductor as opposed to a lower cost air wound coil. This trade-off was made in consideration of test and tune time required to put the air wound coil on frequency. In very large volume applications it may be desirable to replace the C4 and C5 with a single fixed value capacitor and substitute a quality slug tuned coil for L2.

The selection of transistors for the RF and detector stage is not particularly critical and almost any low-noise silicon NPN UHF transistor can be used. The NEC NE680XX (EIAJ 2SC35XX) is ideal because of its high f_t , low noise figure and low cost. Other suitable transistors available in the SOT-23 package include the BFR92 and the MRF941L.

Base bias for the detector stage is provided by quench oscillator U2, a CMOS LMC555 timer integrated circuit. The output from the timer, a 185KHz square wave, is applied to the filter/voltage divider network R15 and R16 and C11. This network shapes the squarewave into a triangle wave with a pk-pk amplitude of 2.5 Volts. The Bias voltage is applied to the base of Q2 through R5.

The ramping trianglewave applied to Q2 varies the gain of the detector until sufficient gain is achieved to sustain oscillation at the RF frequency. The onset of oscillation will occur earlier as the gain is increased by the bias ramping if an RF signal is also present. That is, the time that the detector stage is in oscillation is dependent on the quench signal and the received RF signal strength. The length of time that the detector stage is oscillating effects the average value of current in the collector circuit. This collector current develops a voltage drop across collector resistor R6. The voltage drop across R6 will be proportional to the modulation on the input signal. Figure 3 is shows the collector voltage along with the base signal at the junction of C11 and R5. This detected modulation signal is coupled by C6 to the lowpass network, R12 and C12 which removes most of the large quench signal which will also be present. This lowpass network has a -3dB corner frequency of 3KHz which is a suitably low enough assuming the keyless entry code will be approximately 500 to 1000 bits per second.

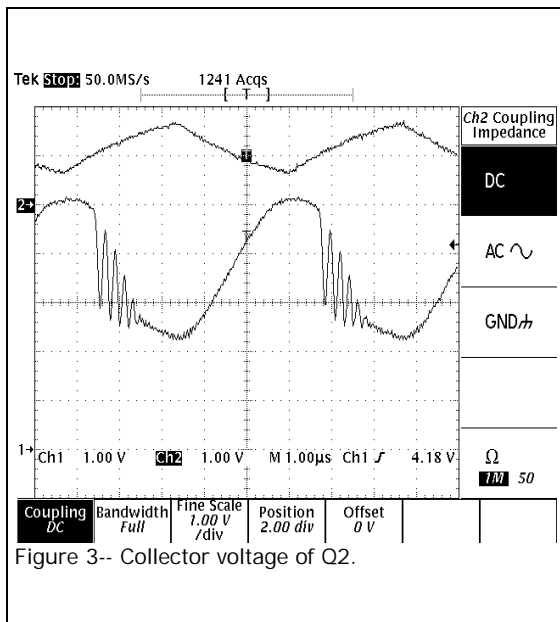


Figure 3-- Collector voltage of Q2.

The first baseband amplifier is U1A and provides approximately a gain of 50 (34dB). The output of U1A is further filter by an additional lowpass filter consisting of R8 and C9 which has a 3dB corner frequency of 16KHz. This should be tailored to your specific transmitter data rate for best bit error rate performance with weak signals. If this lowpass is set to roll-off at too low a frequency then some of the baseband gain will be lost and slow edge transition will cause jitter in the output signal of the next stage. If the frequency roll-off is set too high, then too much quench signal will be present which will also cause jitter in the output signal.

Following the first baseband amplifier and lowpass filter is a voltage comparator which is used to detect the data and convert it into appropriate levels suitable for use by the digital data and clock recovery circuit. This compares the incoming baseband signal against the average of the baseband signal over a relatively long time period. R14 and C10 integrate and hold the dc average of the baseband signal (and noise) with a time constant of 100mS. This signal is applied to the inverting input of the op-amp U1B. The baseband signal is applied to the non-inverting input through R9. A small amount of positive feedback is provided to add hysteresis to the operation of the comparator. This will help reduce noise in the output as the baseband signal transition the threshold value.

It should be pointed out that this data detection scheme can only work properly on a digital data stream that has no dc wander in the average component of the signal. One of the most common data formats that provides no dc wander and a strong timing component is "Manchester"⁶ encoding. Figure 4 shows the actual recovered data out of the comparator

with a -103dBm (1.5uV RMS into 50Ω) signal. This signal, in most cases, will be suitable for directly driving the TTL or CMOS input of any decoder device.

The external quench oscillator, U2, is not connected in the usual manner for a timer IC, that is, threshold (pin 6) and trigger (pin 2) are connected together but discharge (pin 7) is not used. Charging and discharging is accomplished by connecting the pins 2 and 6 to the output (pin 3) through the timing resistor R19. The configuration provides good 50% duty cycle symmetry to the output square wave.

In application where power consumption is critical, the connection and operation of the quench oscillator can help. For example, the output of the quench oscillator, pin 3, can be used to bias on and off the RF amplifier. In this case the base bias resistor of Q1 could be connected to pin 3 of U2. Because the RF stage consumes almost all of the receiver supply current, this modification would cut the power consumption in half. It may also be possible to completely eliminate U2 in cases where the keyless access decoder is a custom ASIC or microprocessor and an extra I/O pin is available. All that is needed is clean 5 Volt pulse capable of sinking and sourcing 0.5mA at the quench frequency applied to pin 1 of J2. Power consumption could be further optimized by tailoring the quench pulse duty cycle along with the changes to the bias filter network R5 and C11.

VR1 is a low drop-out 5 volt regulator that has been included on the receiver circuit board in order to ensure a clean, stable voltage source. This is required because any noise at or below the baseband frequency on the 5 Volt supply will appear as a modulation signal in the output. The 5 Volt regulator could be eliminated if an adequately filtered and stable source of dc where available.

Implementation

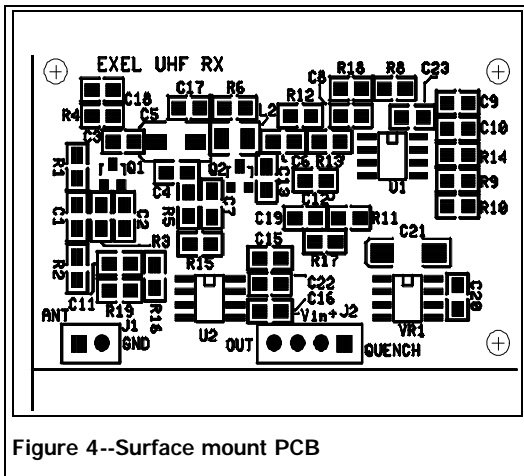


Figure 4--Surface mount PCB

Figure 5 shows the circuits side of the two copper layer receiver printed circuit board. All of the components, with the exception of the connectors, are surface mount technology components. All of the resistor and capacitors are 0805 case sizes. The outside dimensions of the board are 2.10"x 1.25". A smaller board could be fabricated using 0603 case sizes combined with a more conservative layout. The component sizes and board dimensions for this reference design were selected for ease of assembly.

The board material is 0.062" thick FR-4 copper clad on both sides. Nearly of the actual interconnect circuitry is on the component (showing) side of the board. This allows the a solid ground "pour" to be placed on the back side (not shown). Single sided or point-to-point interconnected ground is not recommended for a number of important reasons. For one, the two transistor, Q1 and Q2 are very high frequency devices with f_t well into the GHz region. Without proper ground techniques, these devices will likely be unstable at some very high frequency near their f_t value. In the case of the NE680XX this could easily be in the 7-9GHz and most likely go undetected except for poor receiver sensitivity. Another good reason to use the solid ground pour is for compliance with the unintentional radiation sections of either FCC Part 15 or ETSI-ETS 300 220. Using a two layer board in this manner does not guarantee that the regulatory requirements will be met, but without the ground plane the potential for excessive radiation from the detector will be much greater.

The threshold detector is another critical area to be concerned with. A very high impedance node exists at the junction of R14, C10 and U1B pin 6. Any current leakage from this point due to surface contamination of the board will severely effect the sensitivity of the receiver. It is recommended that after assembly and board wash that a conformal coating be applied to the circuit board. This will ensure that the receivers will continue to provide adequate sensitivity in high humidity applications.

Test and Alignment

The alignment task is very simple because the receiver only has one adjustment. The most accurate way to align the receiver is to use a stable signal generator that has A.M. modulation capability and a calibrated output step/variable attenuator. Set the signal generator for a relatively high level (-40dBm), 1000Hz A.M. modulated 100% (sine wave is OK). With an oscilloscope connected to the data output (J2 pin 4), adjust C5 until the detected a 1000Hz square is observed. Continue to decrease the signal generator attenuator while maintaining a good 1000Hz square wave output from the receiver. The receiver should be able to produce a relative clean output with the generator set to below -100dBm as shown in figure 6.

When bringing up a receiver on a frequency other than 418MHz for the first time, a spectrum analyzer may be helpful in first spotting the frequency of the detector. This can be accomplished by using a small 1 turn loop on the end of a length of coax cable connected to the spectrum analyzer. The loop is brought close to the detector circuit on the receiver board and the analyzer is adjusted until the broad spectrum of the detector is located. The RF spectrum of the detector is quite broad, covering perhaps 1 to 2MHz or so. Component values may have to be changed until the spectrum of the detector is moved close to the desired frequency of operation. Use the procedure above to make the final adjustments. It will be noted that the maximum sensitivity will occur when the frequency spectrum of the detector energy is slight (100-200KHz) below the desired frequency of operation. This is because maximum sensitivity of the detector occurs just as the oscillation starts to build. As the oscillation continues to build through most of the rest of the quench cycle, the bias conditions change in such a way so as to increase the base-collector capacitance and result in lower the sustained frequency of oscillation which is observed on the spectrum analyzer.

When testing, aligning, or for that matter operating a SRR, be cautious of a another SRR operating nearby on the same frequency. The detector of an SRR can radiate enough RF energy to effect the sensitivity an operating frequency of an adjacent SRR. In normal operation this is not likely to occur as more than one receiver in the same location is rare, however, in production testing care should be take to separate test station a sufficient amount so as to minimize any interaction that may occur.

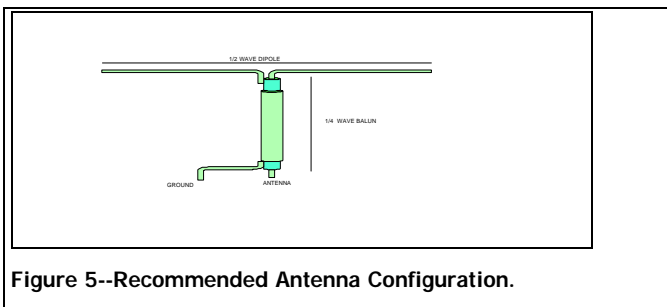


Figure 5--Recommended Antenna Configuration.

Antenna and Shielding

Figure 5 illustrates the recommended antenna configuration for best performance. The antenna consist of a half-wave dipole center fed with a quarter-wave section of coaxial cable. The half-wave section can be typically any solid or stranded AWG 20 gauge copper or copper plated steel wire. The coax

section can be any 50Ω coaxial cable but light weight small diameter cables such as RG-174 will be easier to work with. Calculate the length of the dipole for using the following formula:

$$Ld = \frac{5540}{f(MHz)}$$

Where Ld is the length of the dipole in inches. For 418MHz Ld is 13.25

inches. The quarter wave section in RG-174 can be calculated from

$$Lcoax = \frac{1925}{f(MHz)}$$

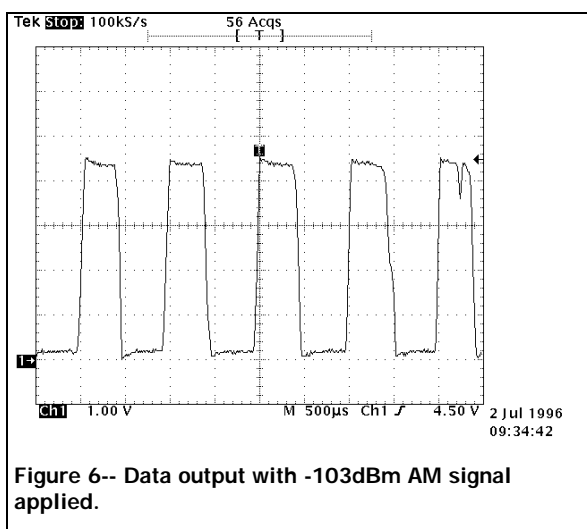
$Lcoax$ is the length of the coax in inches. The antenna and coaxial

feed line should be brought out straight way from the receiver board and any other supporting electronics such as the microprocessor or decoder IC in order to minimize interference from digital clock noise entering the antenna. For best performance the receiver should be surrounded by a metal shield. This will minimize radiation from the detector as well as coupling from the detector and RF amplifier to the antenna.

Range

No discussion of a wireless application can be had without some consideration of the useful and expected range by which the transmitter can be separated from the receiver. In any wireless application range is by far the most difficult performance parameter to predict or guarantee. A number of path loss prediction models have been developed to help the radio engineer estimate range. Some of the best known are the plane-earth propagation equation, the Egli model the JRC method, the Hata formulation and the Okumura method⁷. None of these are very appropriate for keyless entry applications because they are typically based on empirical measurements with modifying factors for ranges of 1 to 10 km between base stations and mobiles. Most of these prediction models assume a mobile will be at a height of 3m and the base station will be at a height of 200m. These are not very useful for keyless entry applications where both receiver and transmitter will be at the same height, usually less than 3m, and separated by not more than 300m.

Shown below is a Mathcad example based on the free space equation with fudge factors for scattering and multipath that can be used by the designer to analyze and reconcile various system parameters in order to determine their effects on the performance of the radio link. This tools can be used to approximate the system performance, the accuracy of your estimate will depend on your ability to assign values to some key parameters .



Specifically, in keyless entry application a number of important factors not usually considered by the path loss prediction models must be taken into account. Among the most difficult parameters to characterize will be:

- The transmitter power into the antenna. In keyless entry applications the transmitter is seldom designed for a specific antenna impedance. So as a result significant mismatch loss errors will occur here.
- The transmit antenna efficiency. Usually the transmitter is a handheld devices with an antenna structure some diminutive fraction of a wave

length. Furthermore, the presence of the hand will further de-tune the transmitter or load the antenna. It can be assumed that the transmit antenna gain is on the order of -10 to -20dBi at best.

- Multipath and scattering losses. These effects can vary widely depending on a variety of circumstances such as; height of transmitter and receiver above ground, absorbing properties of surrounding objects and geometry of reflecting surfaces and the distance separating the receiver transmitter pair. Very deep multipath nulls can occur when the distance is small.
- The effective noise figure and bandwidth of the SRR. These parameters are not part of the path loss prediction models but are important when determining the link margin. These parameters are difficult to measure using direct methods and generally can only be estimated.
- Error performance of the data and clock recover system. Again these parameters are not part of the path loss prediction but knowledge of the signal to noise performance required will be needed in order to assess the link margin. This parameter can be determined by applying a known signal to noise ratio signal to the demodulator logic and characterizing the error rates for a given code and packet size.

Keyless Entry Link Analysis

$$P_{\text{txdBm}} := 6 \quad P_t := .001 \cdot 10^{10} \text{ watt} \quad P_t = 3.981 \cdot 10^{-3} \text{ watt} \quad \text{Transmitter power assumption}$$

$$G_{\text{tdBm}} := 10 \quad G_t := 10^{10} \quad G_t = 0.1 \quad \text{Transmit antenna gain.}$$

$$f := 418 \text{ MHz} \quad \lambda := \frac{300 \cdot 10^6 \text{ m}}{f} \quad \lambda = 0.718 \text{ m} \quad \text{Frequency and wavelength}$$

$$R := 3 \text{ m} \quad R = 10 \text{ ft} \quad \text{For FCC Part 15, range is 3 meters}$$

$$P_d := \frac{P_t \cdot G_t}{4 \pi R^2} \quad P_d = 3.52 \cdot 10^{-6} \text{ watt} \quad \text{m}^2 \quad \text{Power density at a point, } P_d, \text{ due to power transmitted, } P_t, \text{ by a transmitting antenna with a power gain } G_t. R \text{ is the range in meters.}$$

$$E_f := \sqrt{P_d \cdot \pi \cdot \text{ohm}} \quad E_f = 3.325 \text{ mV} \quad \text{m} \quad \text{Electric Field Strength. FCC limit is (section 15.231) is 12.5mV/meter at 3 meters. Transmitter power could be increased or antenna improved.}$$

Now consider the link margin at say 100ft.

$$R_{100} := 100 \text{ ft} \quad R_{100} = 30.48 \text{ m} \quad P_{d100} := \frac{P_t \cdot G_t}{4 \pi R_{100}^2} \quad P_{d100} = 3.41 \cdot 10^{-8} \text{ watt} \quad \text{m}^2$$

$$G_{\text{rdBm}} := 0 \quad G_r := 10^{10} \quad G_r = 1 \quad \text{Receive Antenna Gain}$$

$$A := \frac{\lambda^2 \cdot G_r}{4 \pi} \quad A = 0.041 \text{ m}^2 \quad \text{Antenna effective area}$$

$$P_r := P_{d100} \cdot A \quad P_r = 1.398 \cdot 10^{-9} \text{ watt} \quad \text{Received power in watts}$$

$$P_{\text{rdBm}} := 10 \cdot \log \left(\frac{P_r}{\text{watt}} \cdot 1000 \right) \quad P_{\text{rdBm}} = -58.546 \quad \text{Received power in dBm}$$

$$\text{dBPL} := 10 \cdot \log \left(\frac{P_r}{P_t} \right) \quad \text{dBPL} = -64.546 \quad \text{Path Loss in dB}$$

$$\text{MPL}_{\text{dB}} := 17 \quad \text{Scatt}_{\text{dB}} := 10 \quad \text{Multipath and Scatter Loss in dB}$$

$$\text{NF}_{\text{dB}} := 8 \quad \text{BW}_{\text{rcvr}} := 200 \cdot 10^3 \quad \text{Receiver Noise Figure and Bandwidth}$$

$$\text{MDS} := 174 + 10 \cdot \log(\text{BW}_{\text{rcvr}}) + \text{NF}_{\text{dB}} \quad \text{Minimum Detectable Signal in dBm.}$$

$$\text{MDS} = 112.99 \quad \text{Car}_{\text{noi_ratio}} := P_{\text{rdBm}} - \text{MDS} - \text{MPL}_{\text{dB}} - \text{Scatt}_{\text{dB}} \quad \text{Carrier to Noise Ratio}$$

$$\text{Car}_{\text{noi_ratio}} = 27.444$$

$$\text{Car}_{\text{noi_ratio_req}} := 12 \quad \text{Assume a 12dB carrier to noise ratio is required in order to maintain a 50% successful transmission rate.}$$

$$\text{Link_Margin} := \text{Car}_{\text{noi_ratio}} - \text{Car}_{\text{noi_ratio_req}}$$

Link Margin in dB

d

Conclusion

Using the circuit and layout described you should be able to effectively replicate this design for your application. Modification to this design for operating at other frequencies should present no significant problems and the same layout should be suitable for operation from 50 to over 500MHz.

References:

- ¹ Armstrong, Edwin H., "Some Recent Developments in Regenerative Circuits", Proceedings of the I.R.E. August 1922, pp. 244-260.
- ² Listed below are some of the more significant references on the subject and theory of superregenerative receiver operation:
- Hazeltine, L.A., "Discussion on the Shielded Neutrodyne Receiver", Proceedings of the I.R.E. June 1926, pp. 395-412.
- Robinson, H.A., "Regenerative Detectors", *QST*, Volume 17.2, February 1933, Page 264.
- Ataka, H., "On Superregeneration of an Ultra-Short-Wave Receiver", Proceedings of the I.R.E. August 1935, pp. 841-884.
- Frink, Fredrick W., "The Basic Principles of Superregenerative Reception", Proc. I.R.E, January, 1938
- Fredric Emmons Terman, Sc D., *Radio Engineers Handbook*, McGraw-Hill, First Edition 1943.
- Kalmus, Henry P., "Some Notes on Superregeneration with Particular Emphasis on its Possibilities for Frequency Modulation", Proceedings of the I.R.E., October, 1944, pp. 591-600.
- Strafford, F.R.W., "The Superregenerative Detector: An Analytical and Experimental Investigation", *Journal of the I.E.E.* (London) Part III, No. 21, January 1946, pp. 23-28.
- Tilton, E.P., "Anon-radiating Superregenerative Receiver for Two Meters", *QST*, February 1946, pp. 53-56 and 108.
- Hazeltine FreModyne FM Circuit. Tele-Tech, December 1947, pp. 41, 85, and 86.
- MacFarlane, G.G., and Whitehead, J.R., "The Theory of the Superregenerative Receiver Operated in the Linear Mode.", *Journal of the I.E.E.* (London), Part III, May 1948, pp. 143-157.
- Easton, A., "Superregenerative Detector Selectivity", *Electronics* Volume 19.3 March 1946, Page 154.
- Stockman, H., "Superregenerative Circuit Applications", *Electronics*, Volume 21.2, February 1948, Page 81.
- Wheeler, Harold A., "A Simplified Theory and Design Formulae for Superregenerative Receivers". Wheeler Monograph 3, Wheeler Labs, Inc. Great Neck, N.Y., June 1948.
- Bradley, W.E., "Superregenerative Detection Theory", *Electronics* Vol. 21, Pages 96-89 September 1948.
- Hazeltine, A., Richman D. and Loughlin B.D., "Superregenerator Design". *Electronics*, Vol. 21, pp. 99-102, September 1948.
- Skar, Robert C., "A simplified Analysis of The Superregenerative Receiver", Chamberlain Manufacturing Corporation, December 12, 1948.
- Rina, C.L., "Diode Improves Performance in Superregenerative Circuit", *Electronic Design*, March 14, 1968, Page 230.
- Olson, Hank W6GXN, "Enter the Strange but Useful Blocking Oscillator," *Ham radio*, April, 1969 pp. 45-49.
- Iwakami, A., "Improved Superregenerative Receiver", *Ham Radio*, December 1970, pp. 48-49.
- Rina, C.L., "Optimizing the Superregenerative Detector", *Ham Radio*, July 1972, pp. 32-35.
- Ash, Darrell L., "A Low Cost Superregenerative SAW Stabilized Receiver", *IEEE Trans. on Consumer Electronics*, Vol. CE-33 No. 3, August, 1987.
- Stanley, William D., "Electronic Devices Circuits and Applications", Prentice-Hall, 1989.
- Mitchell & Mitchell, "Introduction to Electronics Design" Prentice-Hall, 1988.
- ³ Eagleware Corporation, 1750 Mountain, Glen Stone Mountain, GA 30087.

⁴ PSPICE is available from a number of software publishers such as MicroSim Corporation, 20 Fairbanks, Irvine CA 92718 or Intusoft, P.O. Box 710, San Pedro CA 90733-0710.

⁵ Compact Software, 201 Mclean Blvd., Paterson, New Jersey, 07504.

⁶ Bellamy, John C., Digital Telephony, John Wiley & Sons, Inc. 1982. 4.3.6 Digital Biphase.

⁷ See either David Parsons, *The Mobile Radio Propagation Channel*, Halsted Press/John Wiley & Sons 1992 or K. Fujimoto & J.R. James, *Mobile Antenna Systems Handbook*, Artech House 1994.

ÿÿÿ sdr 1996